Optimization and characterization of femtosecond laser inscribed in-fiber microchannels for liquid sensing

Graham C. B. Lee, Chengbo Mou, Kaiming Zhou and Kate Sugden

Abstract— **In-fiber microchannels were fabricated directly in standard single mode fiber using the femtosecond laser inscribe and etch technique. This method of creating in-fiber microchannels offers great versatility, since it allows complex three dimensional structures to be inscribed and then preferentially etched with hydrofluoric acid. In addition, inscription does not require a photosensitive fiber; the modification is induced through nonlinear processes triggered by an ultrashort laser pulse. Four in-fiber microchannel designs were experimentally investigated using this technique – microhole, microslot channel along the core, microslot channel perpendicular to the core and helical channel around the core. Each device design was evaluated through monitoring the optical spectral change while inserting a range of index matching oils into each microchannel - an R.I. sensitivity up to 1.55 dB/RIU was achieved in these initial tests. Furthermore, an all femtosecond laser inscribed Fabry-Pérot based refractometer with an R.I. sensitivity of 2.75 nm/RIU was also demonstrated. The Fabry-Pérot refractometer was formed by positioning a microchannel between two femtosecond laser inscribed point-by-point fiber Bragg gratings.**

Index Terms—**Etching, laser machining, liquids, optical device fabrication, optical fiber devices.**

I. INTRODUCTION

In-fiber microchannels enhance the diverse sensing capability of optical fibers to interrogate liquids. Optical fibers are well suited for sensing in harsh environments, which makes them well positioned for sensing hazardous liquids. Similarly, the size and flexibility of optical fibers allows them to be installed in most locations. Optical fibers have previously been used for liquid and gas sensing. Jensen et al. were able to interrogate liquids using photonic-crystal fiber by injecting a fluid into the cladding holes [1]. Liang et al. formed a Fabry-Pérot (FP) interferometer refractive index sensor using a KrF excimer laser and an amplitude phase mask to inscribe two gratings and HF to thin the liquid sensing region of the fiber [2]. Similarly, others have used laser micromachining and etching techniques to fabricate sensors based on micro-wires [3, 4]. Other fiber-tip devices have been used for measuring refractive index [5, 6] and liquid flow [7] . In addition, surface plasmons have also been used to construct sensitive optical fiber hydrogen sensors [8].

The recent development of femtosecond lasers has enabled novel devices to be fabricated into both photosensitive and non-photosensitive optical fibers [9-11]. Femtosecond lasers can create highly accurate and highly localized permanent changes in both opaque and dielectric transparent materials through several non-linear processes [12]. The interaction between a femtosecond laser pulse and a dielectric transparent material can result in a change in refractive index (R.I), birefringence or the creation of a void. The type of modification is selected through the careful control of a vast number of parameters, such as the laser pulse duration, laser fluence and the focusing condition for a given material. In-fiber microchannels fabricated using the femtosecond laser inscribe and etch technique were first demonstrated by Lai et al. in 2006 [13]. Lai and co-workers inscribed and preferentially etched a single 4 μm wide microhole through the fiber core and cladding. This method of creating in-fiber microchannels offers great versatility, since it allows complex three dimensional structures to be directly inscribed with minimal sample preparation. In addition, the final structure of the microchannel can be fine-tuned during the etching process. In this paper, the work of Lai et al. [13] was extended to explore and characterize more complex microchannel designs. Four in-fiber microchannel designs were experimentally investigated in standard single mode fiber using the same inscribe and etch technique. In addition, an all femtosecond laser inscribed FP based refractometer was demonstrated through the inscription of two identical point-by-point fiber Bragg gratings (FBGs) [9] with a microchannel situated in the intrinsic cavity. This paper derives from the paper presented at the 23rd International Conference on Optical Fibre Sensors [14].

II. FEMTOSECOND LASER AND EXPERIMENTAL SETUP

The microchannel and refractometer devices were fabricated using an Amplitude Systèmes s-Pulse HP femtosecond laser that produces sub-500 fs laser pulses at a center wavelength of 1026 nm. The microchannel devices and the FBGs were inscribed using a repetition rate of 100 kHz and 1 kHz respectively. All inscriptions were conducted using

a 100x objective (Mititoyo MPlan Apo NIR Series) with a numerical aperture of 0.5. The approximate FWHM of the laser spot size incident on the samples was 1.5 μm. All devices were fabricated in standard single mode fiber (Corning SMF-28e). The fiber samples were secured to a standard microscope slide with a small section of the acrylate coating removed to facilitate the inscription. A small amount of index matching oil was applied to the area of the fiber where the coating was removed and a cover slip was placed on top of the oil. This fiber mounting configuration was used to reduce the defocusing-induced distortions created by the curvature of the fiber to allow the femtosecond laser beam to remain tightly focused while focusing into the fiber. The microscope slide containing the fiber sample was secured to a motion control system – an X-Y air bearing stage (Aerotech ABL1000) positioned perpendicular to the inscription lens and a mechanical Z stage (Aerotech ANT-4V) for depth control. The motion of the stages was controlled using custom written CNC programs.

III. MICROCHANNEL DESIGN AND LASER INSCRIPTION

Fig. 1. shows the four in-fiber microchannels designs that were tested. The microhole design was implemented by translating the fiber sample through the femtosecond laser beam; the inscription began from bottom of the fiber, through the core and to the top of the fiber. The microslot channels were fabricated through inscribing the desired microslot length in the XY plane and then writing the same microslot layer by layer in the Z plane from the bottom to the top of the fiber. The helical channel around the core was formed by translating the laser beam around the core while maintaining a given distance from the center of the core; two microholes were also fabricated at both ends of the spiral to allow liquids to enter the microchannel. The microhole channel is the simplest of the four designs and the easiest to align prior to laser inscription since the alignment is only dependent on the accuracy in the XY plane. The disadvantage of the microhole channel design is that the interaction volume created in which the liquid and light interact is small compared to the microslot channels. The major drawback of the microslot channel designs, however, is that a large portion of the fiber core is removed, which results in higher losses. In addition, prior to laser inscription, any rotation of the fiber relative to the XY stages must be corrected to ensure the microslot channel runs along or perpendicular to the core. The helical channel is contained within the cladding of the optical fiber but in very close proximity to the fiber core. This ensures minimal losses through the fiber and the interaction length can be controlled by adding more spirals around the core.

The CNC programs were optimized to enable the microhole, microslot channel and helical channel designs to be inscribed in less than 10 seconds (5.5 μm diameter), 90 seconds (50 μm length), and 30 seconds (80 μm length) respectively. The time required to inscribe the mircoslots and helical channels varied depending on the length of the desired device. All microchannel inscriptions were carried out with an approximate pulse energy of 120 – 180 nJ at a 0.2 mm/s translation speed.

Fig. 2. shows the design of a simple FP based refractometer formed by two femtosecond laser inscribed point-by-point FBGs separated by a given length with a microhole positioned between the two gratings. A low 1 kHz repetition rate was used to inscribe the gratings; this allowed a slow stage translation velocity to be used during inscription - to achieve periodically spaced refractive index planes in the fiber core. The center Bragg wavelength was determined by the modified standard Bragg equation:

$$\lambda_B = \frac{2n_e v}{m f_{rr}}$$

Where n_e is the effective refractive index, v is the velocity of the translation stage, m is the order of the grating and f_{rr} is the repetition rate of the laser. Thus, with a fixed n_e, m and f_{rr}, the center Bragg wavelength can be solely controlled by the velocity at which the fiber passes through the laser beam. The response of the FP resonator is primarily controlled by the strength of the two gratings and the cavity length. The free spectral range (FSR) and finesse ($\mathcal{F}$) of the device can be tailored by changing these two properties. The propagation phase shift ϕ induced by the FP cavity can be expressed as:

$$\phi = \frac{4\pi n L_0}{\lambda}$$

Where n is the refractive index of the material, L_0 is the length from the center to center of the two gratings and λ is the wavelength of the source. The maxima of the transmission are obtained when the phase shift is $\phi = 2\pi m$ (where m is an integer) to form:

$$\lambda_m = \frac{2nL_0}{m}$$

Therefore, the FSR which is $\Delta\lambda$ between two successive transmitted or reflected maxima or minima can be expressed as:

$$\Delta\lambda_{FSR} = \lambda_m - \lambda_{m+1}$$

$$\Delta\lambda_{FSR} = 2nL_0 \left(\frac{1}{m} - \frac{1}{m+1} \right)$$

If m is large, this can be simplified to:

$$\Delta\lambda_{FSR} \simeq \frac{\lambda^2}{2L_0 n}$$

The $\mathcal{F}$ of an FP resonator is defined as the ratio of its FSR and FWHM bandwidth [15] and describes the contrast between the maxima and minima of the transmitted waveform. Where $\mathcal{R}$ is the reflectivity of the two gratings. A high finesse would produce very sharp peaks.

An FP refractometer device with $L_s = 1$, L_1 and $L_2 = 2$ mm is presented in this paper. The two identical gratings shown in Fig. 6a. are second order 1550 nm Bragg gratings, inscribed with 250 nJ per pulse at a 1 kHz repetition rate. The calculated

FSR = 0.278 nm. A 8 μm microhole positioned in the intrinsic cavity was inscribed with 850 nJ pulse energy at 100 kHz repetition rate.

IV. HF ETCHING

After femtosecond laser inscription, each microchannel device was etched in a 5 % hydrofluoric acid solution assisted by an ultrasonic bath, the approximate etch time required for each device were: microhole (25 minutes), microslots (10 to 60 minutes) and helix (60 minutes). The fully etched microchannel devices are shown in the microscope images presented in Fig. 3. The size of the final etched microchannel devices is dependent the number of laser passes, pulse energy delivered and inscription speed for a given lens and repetition rate. After laser inscription, the final microchannel dimensions can be slightly tuned through making small adjustments to the etch time.

V. REFRACTIVE INDEX MEASUREMENTS

The R.I. sensitivity of each microchannel device was evaluated by immersing each microchannel in a range of index matching oils (Cargille Labs) while measuring the optical transmission losses, the results are shown in Fig. 4. A total of twelve index matching oils were tested in each channel – 1.300 to 1.456. With reference to Fig. 5. for R.I. oils from 1.30 to 1.38, the single spiral microchannel was the least sensitive device with a sensitivity of 0.51 dB/RIU, due to the microchannel being confined only to the cladding. Whereas the microslot channel perpendicular to the core was the most sensitive at 1.55 dB/RIU. It should be noted that a 0.14 dB transmission loss was observed through the microslot channel perpendicular to the core when the channel was filled with a 1.30 R.I. oil, whereas the transmission loss was negligible through the single spiral microchannel filled with the same index oil.

The FP refractometer, featuring a microhole had a R.I. sensitivity of 2.75 nm/RIU and measures a wavelength shift as opposed to a transmission loss. A section of the point-by-point inscribed FBG and the spectral response of the FP refractometer is shown in Fig. 6b.

VI. DISCUSSION

Overall, all four microchannel designs would make suitable refractometer sensors. The limited linear sensing range for this type of sensor device, however, may be an issue in some applications. The helical channel devices showed the most promise; with further development it should be possible to increase the sensitivity and reduce the losses in this design. The helical channel proved to be the most difficult to fabricate because the inscription was very sensitive to the alignment on all three axes. In addition, cleaning the helical channels required extra effort since the liquid would often reside in the bends of the channel. Nonetheless, a long helical channel with multiple spirals in close proximity to the core would create a very sensitive refractive index sensor with minimal losses.

All microchannel devices discussed in this paper were inscribed using a 100 kHz laser repetition rate. Little to no difference was observed between devices written using 1 kHz

with the same average power as at 100 kHz. Similarly, the required pulse energy was not particularly significant, a broad range of values from 100 – 600 nJ per pulse at 100 kHz repetition rate were capable of creating clean and well defined channels. Too much energy, however, boiled the oil and created bubbles around the fiber. Bubbles can cause an uneven layer of oil around the fiber, which could result in an uneven inscription. As a general rule of thumb, the pulse energy was chosen based on observing the fully inscribed structure under a transmission microscope prior to etching.

A fully etched microhole device normally featured high aspect ratio walls with a small taper at the top surface. In Fig. 3. a small 0.035° taper angle over the 125 μm diameter of the fiber can be observed. This taper angle was typically observed in all etched channels due to the method used to inscribe the devices. The fiber edge closest to the machining lens in the inscription setup would normally have a wider channel width when compared to the channel width at the bottom fiber edge. This was a result of the defocusing of the laser beam spot as it penetrated deeper into the fiber. It would be possible to reduce this effect by changing the mounting configuration and by employing a fiber rotator. For example, if the fiber was held at both ends, inscription can be done from the center of the core to the top of the fiber. Subsequently, the fiber can be rotated 180° and the other half of the fiber can be inscribed in the same way. This would create a more symmetrical channel but at the cost of a more elaborate setup.

Equally, the fully etched microslot channels along and perpendicular to the core shown in Fig. 3b and c typically featured a similar taper on the walls as seen with the microhole devices. Under an optical transmission microscope, the walls of the microslot channels appeared to be very smooth and can be further improved through etching for an additional two or three minutes. Unfortunately, it is difficult to accurately measure the side wall roughness without breaking the microslot channel and profiling the surface with an AFM. The ability to regulate the roughness of the channel walls would be very advantageous for some microfluidic applications [16-18]. The accuracy of the etch time required for the microslot channels along and perpendicular to the core were much more critical than for the microhole devices because of the difference in etch rates between the core and the cladding. The etch rate of the germania-doped core is approximately 11.5 times faster than the pure silica cladding [19]. For the microhole devices, the difference in etch rates did not play a major role because the inscription area was carefully controlled and the etching process could be stopped as soon as the entire channel had been removed. For the microslot devices, however, the larger area that had to be removed by the acid required a longer etching time and the additional exposure to the acid meant that the difference in etch rates played a much greater role. Typically, a microslot that had been inscribed with a given length would produce an etched device with an additional 8-10 μm in length caused by the effective material modified area. Of course, the difference between desired and resultant length can be account for by including an offset in the CNC program.

The helical channel around the core devices required the longest HF acid exposure due to the geometry of the inscribed structure. The ultrasonic bath was essential in achieving a

thorough etch; a static HF acid fluid could not penetrate deep inside of the channels. The dark areas in the channel seen in Fig. 3d. are a result of areas not fully filled with the index matching imaging oil.

VII. CONCLUSION

Femtosecond laser inscribed and hydrofluoric etched microchannel designs for liquid sensing has been demonstrated. The fabrication parameters have been optimized to produce high quality devices and a more complex design space has been explored to enable the fabrication of 3D devices. An R.I. sensitivity up to 1.55 dB/RIU was achieved using the microslot channel perpendicular to the core. A simple FP based refractometer with a microslot channel perpendicular to the core yielded an R.I. sensitivity of 2.75 nm/RIU. Further investigations are underway to incorporate and test the other three microchannel types in the FP refractometer design. The FP device was made using a single laser platform allowing the FBGs and slot to be accurately positioned relative to each other. Further trials are required to determine the usability of the microchannel devices for gas sensing.

REFERENCES

[1]   J. B. Jensen, L. H. Pedersen, P. E. Hoiby, L. B. Nielsen, T. P. Hansen, J. R. Folkenberg, *et al.*, "Photonic crystal fiber based evanescent-wave sensor for detection ofbiomolecules in aqueous solutions," *Opt. Lett.,* vol. 29, pp. 1974-1976, 2004.

[2]   W. Liang, Y. Huang, Y. Xu, R. K. Lee, and A. Yariv, "Highly sensitive fiber Bragg grating refractive index sensors," *Applied Physics Letters,* vol. 86, pp. -, 2005.

[3]   R. M. André, S. Pevec, M. Becker, J. Dellith, M. Rothhardt, M. B. Marques, *et al.*, "Focused ion beam post-processing of optical fiber Fabry-Perot cavities for sensing applications," *Optics Express,* vol. 22, pp. 13102-13108, 2014/06/02 2014.

[4]   S. Pevec and D. Donlagic, "Miniature micro-wire based optical fiber-field access device," *Optics Express,* vol. 20, pp. 27874-27887, 2012/12/03 2012.

[5]   P. Nath, H. K. Singh, P. Datta, and K. C. Sarma, "All-fiber optic sensor for measurement of liquid refractive index," *Sensors and Actuators A: Physical,* vol. 148, pp. 16-18, 11/4/ 2008.

[6]   S. F. O. Silva, O. Frazão, P. Caldas, J. L. Santos, F. M. Araújo, and L. A. Ferreira, "Optical fiber refractometer based on a Fabry-Pérot interferometer," *Optical Engineering,* vol. 47, pp. 054403-054403-5, 2008.

[7]   V. Lien and F. Vollmer, "Microfluidic flow rate detection based on integrated optical fiber cantilever," *Lab on a Chip,* vol. 7, pp. 1352-1356, 2007.

[8]   C. Perrotton, R. J. Westerwaal, N. Javahiraly, M. Slaman, H. Schreuders, B. Dam, *et al.*, "A reliable, sensitive and fast optical fiber hydrogen sensor based on surface plasmon resonance," *Opt. Express,* vol. 21, pp. 382-390, 2013.

[9]   A. Martinez, M. Dubov, I. Khrushchev, and I. Bennion, "Direct writing of fibre Bragg gratings by femtosecond laser," *Electronics Letters,* vol. 40, pp. 1170-1172, 2004.

[10]   G. N. Smith, T. Allsop, K. Kalli, C. Koutsides, R. Neal, K. Sugden, *et al.*, "Characterisation and performance of a Terfenol-D coated femtosecond laser inscribed optical fibre Bragg sensor with a laser ablated microslot for the detection of static magnetic fields," *Optics Express,* vol. 19, pp. 363-370, 2011/01/03 2011.

[11]   G. C. B. Lee, K. Kalli, C. Koutsides, M. Komodromos, and K. Sugden, "Femtosecond laser microstructuring through optical fibre end faces: inscription of surface gratings and sub-surface splitters," in *OFS 2012 22nd International Conference on Optical Fiber Sensors*, Beijing, China, 2012, pp. 842111-842111-4.

[12]   K. M. Davis, K. Miura, N. Sugimoto, and K. Hirao, "Writing waveguides in glass with a femtosecond laser," *Opt. Lett.,* vol. 21, pp. 1729-1731, 1996.

[13]   Y. Lai, K. Zhou, L. Zhang, and I. Bennion, "Microchannels in conventional single-mode fibers," *Opt. Lett.,* vol. 31, pp. 2559-2561, 2006.

[14]   G. C. B. Lee, C. Mou, K. Zhou, and K. Sugden, "Optimization and characterization of femtosecond laser inscribed in-fiber microchannels for liquid sensing," in *OFS 2014 23rd International Conference on Optical Fiber Sensors*, Santander, Spain, 2014, pp. 915743-915743-4.

[15]   B. E. A. Saleh and M. C. Teich, *Fundamentals of Photonics*, 2nd ed. Hoboken, New Jersey: Wiley, 2007.

[16]   B. Zhao, J. S. Moore, and D. J. Beebe, "Surface-Directed Liquid Flow Inside Microchannels," *Science,* vol. 291, pp. 1023-1026, February 9, 2001 2001.

[17]   Z.-X. Li, "Experimental study on flow characteristics of liquid in circular microtubes," *Microscale Thermophysical Engineering,* vol. 7, pp. 253-265, 2003/01/01 2003.

[18]   P. Truman, P. Uhlmann, and M. Stamm, "Monitoring liquid transport and chemical composition in lab on a chip systems using ion sensitive FET devices," *Lab on a Chip,* vol. 6, pp. 1220-1228, 2006.

[19]   D. J. Markos, B. L. Ipson, K. H. Smith, S. M. Schultz, R. H. Selfridge, T. D. Monte, *et al.*, "Controlled Core Removal from a D-Shaped Optical Fiber," *Appl. Opt.,* vol. 42, pp. 7121-7125, 2003.
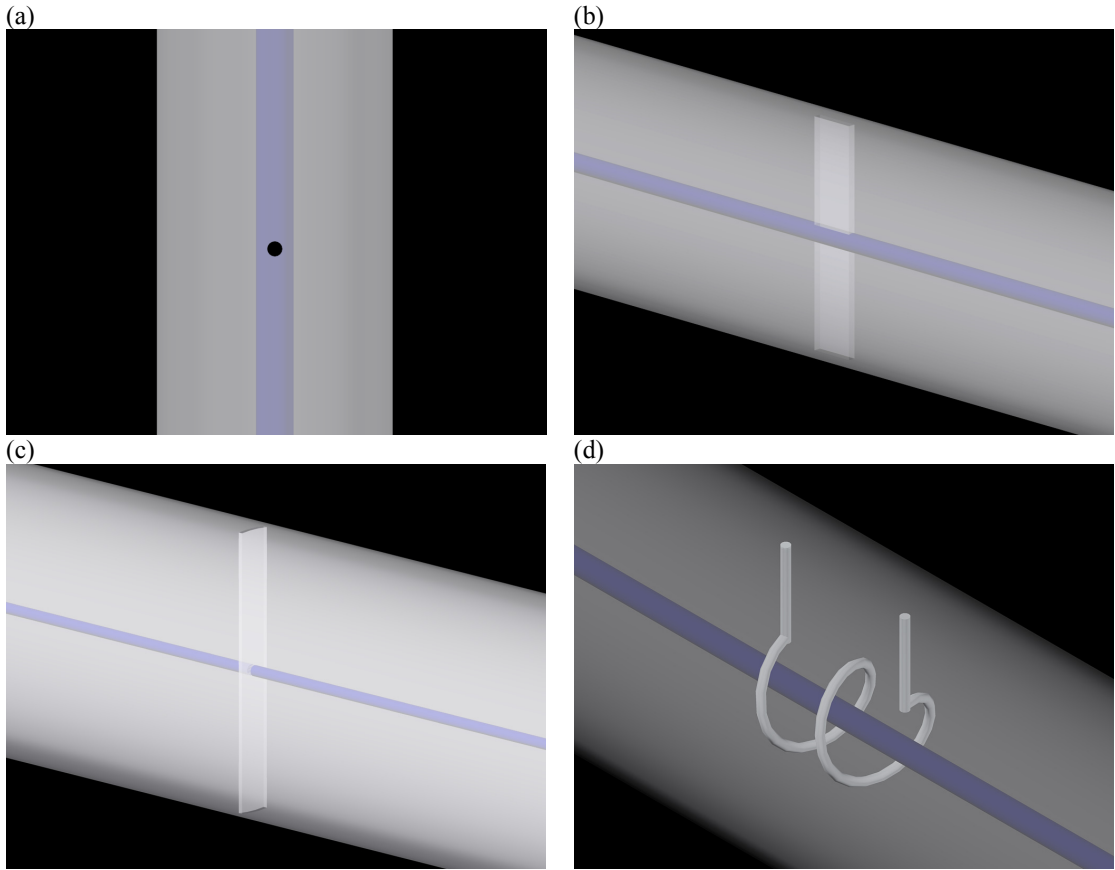
Fig. 1. CAD render of the in-fibre microchannel designs: (a) microhole, (b) microslot channel along the core, (c) microslot channel perpendicular to the core and (d) helical channel around the core.
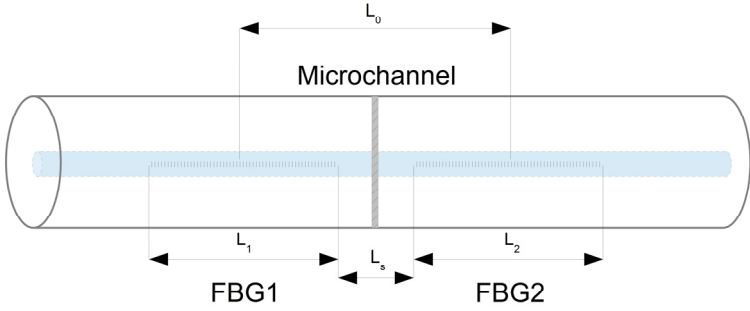

Fig. 2. FP resonator in standard SMF formed by two FBGs (FBG1 and FBG2), L_1 and L_2 are the respective lengths of the gratings. L_0 is the cavity length (center to center length of the two gratings). L_s is the separation between the last grating plane of FBG1 and first grating plane of FBG2.
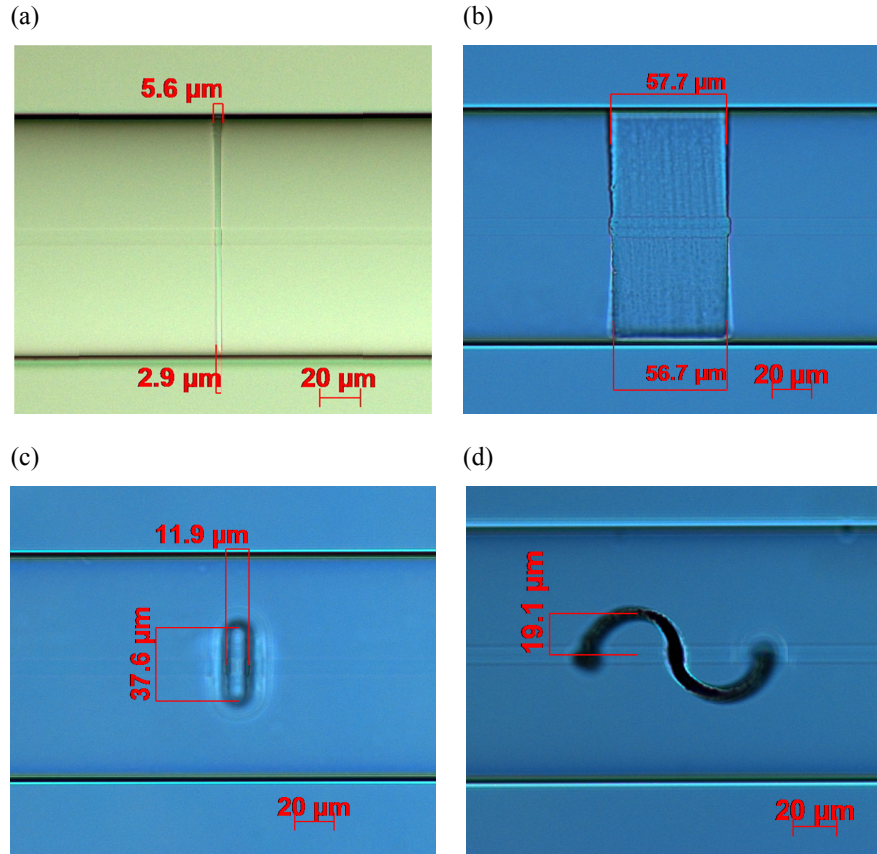
Fig. 3. Femtosecond laser inscribed and etched microchannel devices – (a) microhole, (b) microslot channel along the core (c) microslot channel perpendicular to the core and (d) single spiral channel around the core.
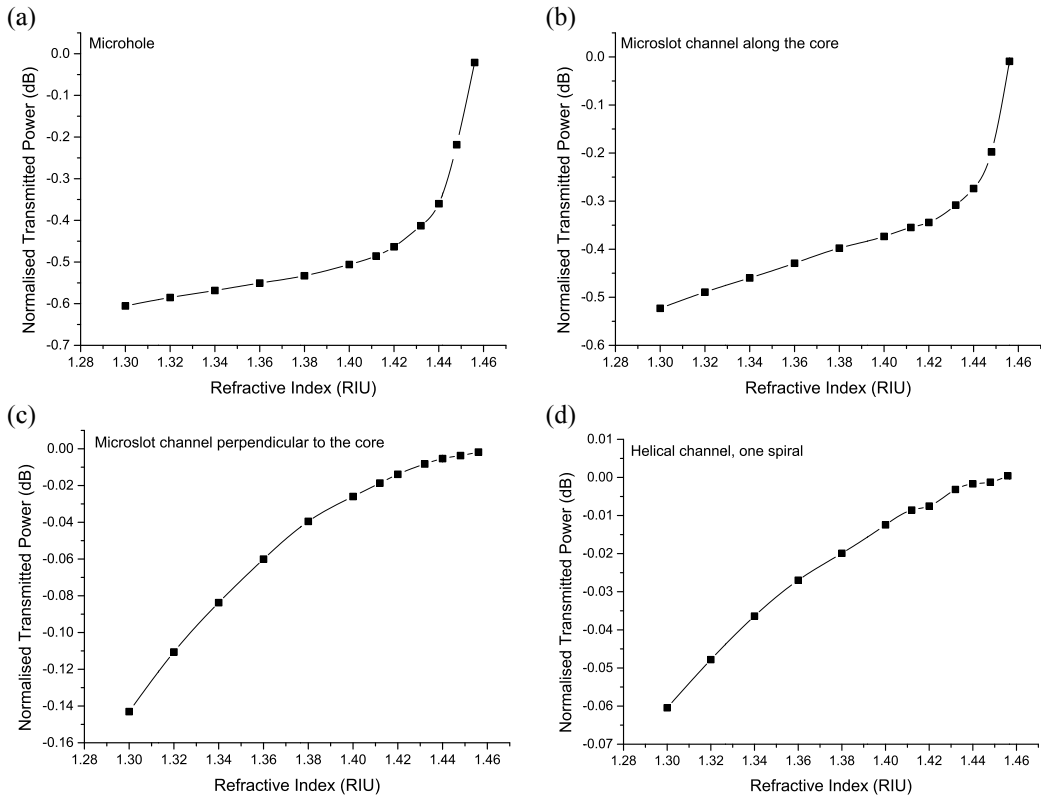
Fig. 4. Averaged and normalised optical transmission losses measured with index matching oils in a (a) microhole with a 5.6 µm channel diameter in the core, (b) microslot channel along the core with a 57 µm slot length, (c) microslot channel perpendicular to the core with a 11.9 µm interaction length in the core and (d) helical channel with one spiral at 19.1 µm from the center of the core. Power measurements collected using a LUNA Optical Vector Analyzer (data taken at 1563 nm) with a 1.25 pm wavelength resolution.
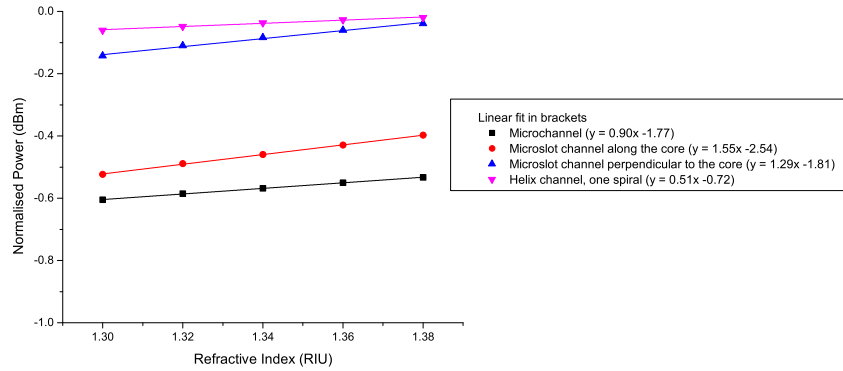

Fig. 5. Linear relationship between the optical transmission losses and the index matching oils 1.300 to 1.380 for the in-fibre channels. Equation of the linear fit is shown on the right hand side.
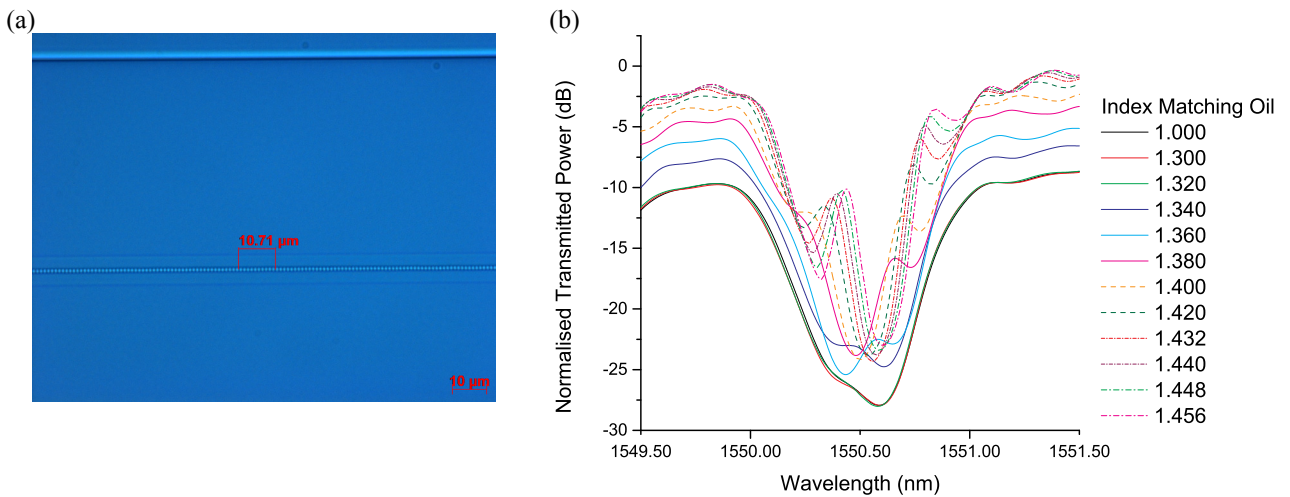

Fig. 6. (a) Optical microscope image showing a section of the point-by-point 2nd order 1550 nm grating; measurement shows the length of 10 grating planes. (b) Fabry–Pérot based refractometer - averaged and normalized optical transmission losses measured with index matching oils in the microhole. Measured using a LUNA Optical Vector Analyzer with a 1.25 pm wavelength resolution.